Vehicle Energy/Emissions Estimation Based on Vehicle Trajectory Reconstruction Using Sparse Mobile Sensor Data

Xiaonian Shan, Peng Hao, *Member, IEEE*, Xiaohong Chen, Kanok Boriboonsomsin, *Member, IEEE*, Guoyuan Wu, *Senior Member, IEEE*, and Matthew J. Barth, *Fellow, IEEE*

***Abstract*— Microscopic vehicle emissions models have been well developed in the past decades. Those models require second-by-second vehicle trajectory data as a key input to perform vehicle energy/emissions estimation. Due to the omnipresence of mobile sensors such as floating cars, real-world vehicle trajectory data can be collected in a large scale. However, most large-scaled mobile sensor data in practice are sparse in terms of sampling rate due to the consideration in implementation cost. In this paper, a new modal activity framework for vehicle energy/emissions estimation using sparse mobile sensor data is presented. The valid vehicle dynamic states are identified including four driving modes, named acceleration, deceleration, cruising, and idling. The best valid vehicle dynamic state with the largest probabilities is selected to reconstruct the second-by-second vehicle trajectory between consecutive sampling times. Then vehicle energy/emissions factors are estimated based on operating mode distributions. The proposed model is calibrated and validated using the Next Generation Simulation's dataset, and shows better performance in vehicle energy/emissions estimation compared with the linear interpolation model. Sensitivity analysis is performed to show the model accuracy with different time intervals. This paper provides a new methodology for vehicle energy/emissions estimation and extends the application area of sparse mobile sensor data.**

***Index Terms*— Modal activity, vehicle trajectory reconstruction, vehicle energy/emissions estimation, maximum likelihood estimation.**

I. Introduction and Motivation

IN MANY urban areas, vehicle emissions have been recognized as one of the major contributors to air pollutions that can pollute the environment and cause public health issues. Reducing vehicle emissions from motorized transportation areas plays a significant role in improving urban air quality and decreasing atmospheric greenhouse gases. Microscopic vehicle emissions models, such as Comprehensive Model Emissions Model (CMEM) [1] and MOtor Vehicle Emission Simulator (MOVES) [2], have been well developed to calculate vehicle energy consumption and emissions precisely. However, these models require second-by-second vehicle trajectory data as a key input to perform vehicle energy/emissions estimation.

In recent years, due to the technical advances in mobile devices, large scale vehicle trajectory data are available through mobile sensors, such as probe vehicles equipped with Global Positioning System (GPS). Data collected by GPS include coordinated universal time, global positions (i.e., latitude, and longitude), and speeds of vehicles at a certain frequency. For large-scale data collection efforts, the data sampling rate may range from 10 s to 60 s in order to manage the costs of data transmission and storage. For example, almost 50,000 taxi cabs and 16,000 buses in Shanghai, China, are equipped with GPS technology and transmit their position and speed information to the city's traffic management center at a certain time interval from 10 s to 30 s. Thus, before sparse mobile sensor data can be used in vehicle energy/emissions estimation, it is necessary to first reconstruct the vehicle trajectories to a time resolution (e.g., second-by-second) as a key input to the micro vehicle emissions models or other aspects of traffic modeling.

Many researchers have been aware of the above challenge and have actively investigated the tradeoffs between sampling rate of mobile sensor data and reliability of traffic modeling. Quiroga and Bullock suggested that vehicle trajectory data sampling period should be around 1 s to minimize errors in computation of average speeds and travel times along highway segments [3]. Liu *et al.* [4] developed two delay measurement algorithms at intersections corresponding to high-frequency probe data (at 5 s time interval) and lower-frequency data (from 10 s to 60 s). Herring *et al.* [5] proposed a probabilistic modeling framework for estimating and predicting arterial travel time distributions using sparsely observed probe vehicle with 60 s time interval. Wang *et al.* [6] proposed a hidden Markov model for urban scale traffic estimation using floating car data in order to overcome the problem of data sparseness. Liu *et al.* [7] reconstructed the vehicle trajectories to estimate vehicle emission factors based on taxi GPS data and MOVES revised emission inventory in Shanghai, China. Zhou *et al.* [8] constructed detailed vehicle trajectories

Manuscript received December 5, 2017; revised March 28, 2018; accepted April 7, 2018. Date of publication May 11, 2018; date of current version January 31, 2019. This work was supported by the National Natural Science Foundation of China under Grant 71734004. The Associate Editor for this paper was R. Trasarti. *(Corresponding author: Xiaohong Chen.)*

X. Shan and X. Chen are with the Key Laboratory of Road and Traffic Engineering of the Ministry of Education, Tongji University, Shanghai 201804, China (e-mail: 3ashan@tongji.edu.cn; chenxh@tongji.edu.cn).

P. Hao, K. Boriboonsomsin, G. Wu, and M. J. Barth are with the Center for Environmental Research and Technology, University of California at Riverside, Riverside, CA 92507 USA (e-mail: haop@cert.ucr.edu; kanok@cert.ucr.edu; gywu@cert.ucr.edu; barth@ee.ucr.edu).

Digital Object Identifier 10.1109/TITS.2018.2826571

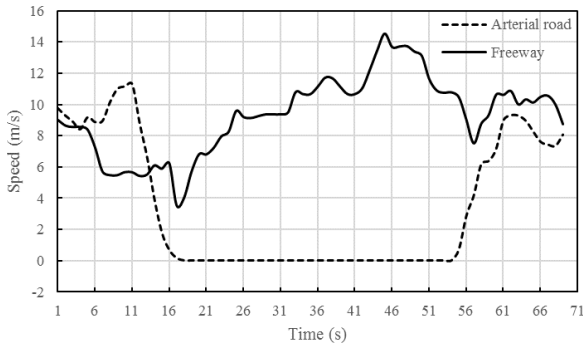

Fig. 1. Vehicle driving trajectory on different road types.

and time-depend speed profiles for vehicle energy/emission estimation based on mesoscopic traffic simulation output data. Zegeye *et al.* [9] proposed a general framework to integrate macroscopic traffic flow models and microscopic emission and fuel consumption models through constructing vehicle trajectories. Recently, due to the limitation of linear interpolation model, Hao *et al.* [10] proposed a stochastic model to estimate the second-by-second vehicle trajectories and evaluate the link travel time distribution using sparse mobile sensor data on arterial road. Further, vehicle energy and emissions characteristics on arterials were estimated using MOVES based on the reconstructed vehicle trajectories [11].

In Hao's model, a strong assumption is that the driving modes of a vehicle must evolve with a certain pattern, i.e. idle → acceleration → cruise → deceleration → idle → ... periodically [10], [11]. It is reasonable when a vehicle is traveling on an arterial road with frequent stop-and-go maneuver at traffic signals and during congestions. However, when a vehicle is traveling on a freeway, the vehicle may decelerate only to some low speeds other than zero and accelerate back to free-flow speed. Even driving on an arterial road, a vehicle can also accelerate or decelerate to a certain speed, rather than free-flow speed or zero, see Fig. 1. Such non-stop speed oscillations inspire a new modal activity-based model in this study to reconstruct vehicle trajectories for vehicle energy/emissions estimation.

Therefore, the primary objective of this study is to propose a new framework of modal activity-based vehicle energy/emissions estimation using sparse mobile sensor data based on reconstructed trajectories. The rest of this paper is organized as follows: The proposed methodology is introduced for vehicle trajectory reconstruction in the following section. This method is further applied for purpose of vehicle energy/emissions estimation. Model calibration is conducted using freeway and arterial road datasets from the Next Generation Simulation (NGSIM) program [12], [13]. Results of numerical experiments are presented and discussed using the other period datasets from NGSIM in section of numerical experiments. The paper ends with brief concluding remarks along with future works.

II. Methodology

Methods for reconstructing vehicle trajectories using sparse mobile sensor data are developed in this section. We firstly describe the model assumptions of modal activity-based vehicle trajectory reconstruction, and identify valid vehicle dynamic states. Vehicle trajectory reconstruction for acceleration/deceleration mode is then introduced. Besides, speed oscillation effect of cruising modal is integrated in our model framework.

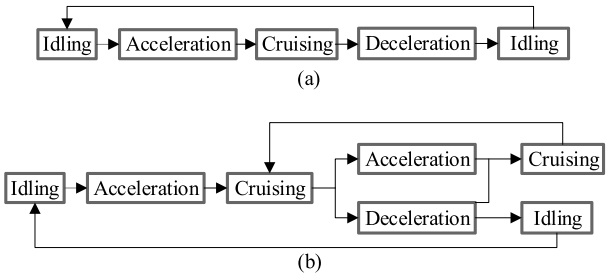

Fig. 2. Vehicle driving modes assumption on different road types.

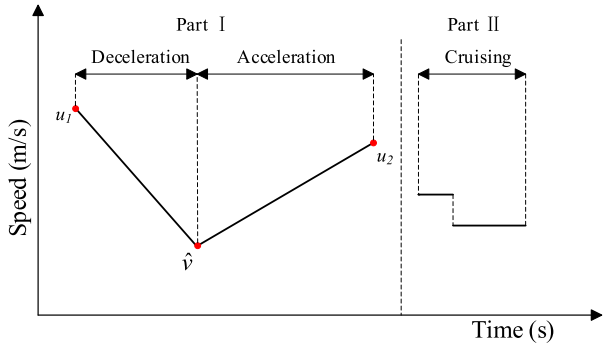

Fig. 3. Problem formulation of vehicle trajectory reconstruction.

A. Model Assumption

Modal activities of vehicles can be categorized into four classes: idling, acceleration, cruising and deceleration. For the vehicles on urban arterial roads [10], [11], cruising mode is considered as a high-speed state between acceleration and deceleration mode, see Fig. 2(a). In this paper, we assume that the vehicle may keep its speed for a while within the acceleration or deceleration process (i.e., acceleration → cruising → acceleration). Under heavy traffic congestion, the driver may control its speed to avoid stop-and-go maneuver. The vehicle may decelerate early, cruise at low speed and then accelerate to catch up leading vehicles. In general, the vehicle may cruise at any speed below speed limit, including zero if we regard idling mode as a special cruising condition, see Fig. 2(b).

Based on the relaxed assumption above, we identify the type, time and distance of each modal activity based on the location and speed information of a sparse mobile data pair with certain sampling rate. Two major issues are discussed in this section: 1) identification of inflection speed point which is defined as the inflection point in the trajectory between an acceleration and a deceleration process or vice versa; and 2) determination of modal travel time and distance.

As shown in Fig. 3 and Fig. 4, for a certain sparse mobile sensor data pair, the starting speed (u_1), ending speed (u_2), time interval (Δt) and total traveling distance (Δd) are given. The key objective in trajectory estimation is to

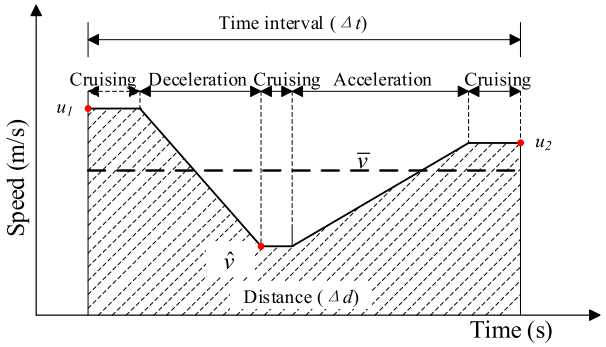

Fig. 4. Modal transition assumption.

identify modal activity sequence and assign appropriate travel time and distance to each mode. We assume that there is at most one inflection speed point ($\hat{v}$) between a data pair based on observations. The value of the inflection speed point should be identified before estimating times and distances that the vehicle takes under acceleration and deceleration modes, as shown in the part I of Fig. 3. We assume that vehicles can cruise at any speed between the maximum speed and the minimum speed, resulting in one or multiple cruising mode segment, as shown in the part II of Fig. 3. The crucial challenge is to estimate the time and distance for each cruising segment and assign them to the adequate position of the vehicle trajectory.

Furthermore, some sequences, such as deceleration → cruising → acceleration, are allowed in our model. However, we ignore some sequences that are statistically trivial in real world to simplify the model because of the extremely low probability of occurrence during a certain time interval based on filed observations, such as acceleration → cruising → acceleration or deceleration → cruising → deceleration. For example, statistics on NGSM U.S. 101 dataset shows that if the sampling time interval is 10 s, almost all cruising processes occur at the start/end of a time interval, or between acceleration and deceleration modes with the inflection speed point. The percentage of an intermediate cruising process within the process of acceleration (i.e. acceleration → cruising → acceleration) is 2.7%. With in the process of deceleration, the percentage is only 0.6%. We assume that modal transition only happens at the starting speed, ending speed and inflection speed, which means cruising modal only happens at these three speed points, see Fig. 4.

B. Vehicle Dynamic State Identification

For a modal activity-based trajectory estimation problem, the vehicle dynamic state is an essential bridge between GPS data and estimated second-by-second trajectories, as it includes all key information for trajectory reconstruction. For the arterial problem, the vehicle dynamic state is determined by the modal activity sequence (i.e., **M**), free flow speed (i.e., U), along with the travel time (denoted as $\mathbf{T}_i$) and distance (denoted as $\mathbf{X}_i$) of each mode. The free flow speed is important for the arterial case as it is always considered as the average speed of cruising mode, the starting speed of deceleration mode, ending speed of the acceleration mode. For the freeway scenario, as the mode transition may happen at any speed below the speed limit, we relax that assumption. A modal transition speed vector **V** is introduced to substitute U. The first element of **V** is the starting speed (u_1) of the sparse data pair, and the last one is the ending speed (u_2). The elements in between are the speeds at all modal transition sequentially. It is apparent that **V** has one more element than **M**.

TABLE I
PROBABILITY OF DIFFERENT MODAL ACTIVITY SEQUENCE

P(**M**=**m**)	$\bar{v} > u_{\max}$	$\bar{v} < u_{\min}$	$\bar{v} \in [u_{\min}, u_{\max}]$
$\mathbf{M} = [S3,S4,S3,S2,S3]^T$	0	1	0.25
$\mathbf{M} = [S3,S2,S3,S4,S3]^T$	1	0	0.25
$\mathbf{M} = [S3,S2,S3]^T$	0	0	0.25
$\mathbf{M} = [S3,S4,S3]^T$	0	0	0.25

For a given vehicle trajectory, there exists a certain vehicle dynamic state {**m**, **v**, **t**, **x**}. We denote idling mode as S1, acceleration mode as S2, cruising mode as S3 and deceleration mode as S4 to show **M**. For the example case in Fig. 4, $\mathbf{M} = [S3,S4,S3,S2,S3]^T$ and $\mathbf{V} = [u_1, u_1, \hat{v}, \hat{v}, u_2, u_2]^T$. **T** and **X** are the time and distance for the five modal activities in **M** respectively. Similar as the arterial model in [10], we assume a truncated normal distribution for the acceleration/deceleration pace (i.e., the reciprocal of the average acceleration rate). We also assume the distance under acceleration/deceleration mode follows another truncated normal distribution factored by the modal travel time and speed. For the cruising or idle mode, the modal travel time and distance are assumed to be uniformly distributed. Note that in this study idle is regarded as a special cruising driving mode. Furthermore, a certain driving mode of the sequence may not exist, the travel time and distance of such mode is equal to zero.

The vehicle dynamic state (**M**) is dependent on the relationship among u_1, u_2 and $\bar{v}$ (average speed $\bar{v} = \Delta d/\Delta t$). Note that if the vehicle only experiences a single acceleration or deceleration process in a certain time interval, the average speed must fall between the starting and ending speed. Therefore, if the value of $\bar{v}$ is not between u_1 and u_2, i.e. $\bar{v} > u_{\max} = \max(u_1, u_2)$ or $\bar{v} < u_{\min} = \min(u_1, u_2)$, there must be an inflection speed point. On the contrary, if the value of $\bar{v}$ is between u_1 and u_2, the existence of the inflection speed point is undefined. In this paper we simply assume that the probability of **M** is equally distributed when there is no extreme speed point. Obviously, if there is an extreme speed, the length of **M** is 5; and the length of **M** is 3 when there is no extreme speed. Probabilities of **M** are shown in Table I.

After determining vehicle dynamic states (**m**), the lengths of **v**, **t** and **x** could be also determined. Then probability of **V** could be calculated using equation (1). The prior probability of the extreme speed $\hat{v}$ will be explored in the next subsection. Noted that we discretize the continuous quantity $\hat{v}$ with the interval of 0.28 m/s to calculate the probability of the inflection

speed.

$$P(\mathbf{V}=\mathbf{v}|\mathbf{M}=\mathbf{m})=\begin{cases}P(\hat{v}), & \hat{v}\geq 0,\ K=5;\\ 1, & K=3.\end{cases} \tag{1}$$

Furthermore, to a certain vehicle state, the travel time and distance are independent of the time and distance of other modes. So the general form of the conditional probability density functions for T_{i} and X_{i} are:

$$\begin{aligned}P(T_i=t_i|\mathbf{V}=\mathbf{v},\mathbf{M}=\mathbf{m}) &= f_T(t_i;\ v_i,\ v_{i+1},m_i);\\ P(X_i=x_i|T_i=t_i,\mathbf{V}=\mathbf{v},\mathbf{M}=\mathbf{m}) &\\ = f_X(x_i;\ t_i,\ v_i,\ v_{i+1},m_i).&\end{aligned} \tag{2}$$

Finally, the probability of a vehicle dynamic state can be reformulated as the product of probabilities of multiple independent events:

$$\begin{aligned}P(\mathbf{M}=\mathbf{m},\mathbf{V}=\mathbf{v},\mathbf{T}=\mathbf{t},\mathbf{X}=\mathbf{x})&\\ =\prod_i P(X_i=x_i|T_i=t_i,\mathbf{V}=\mathbf{v},\mathbf{M}=\mathbf{m})&\\ \cdot\prod_i P(T_i=t_i|\mathbf{V}=\mathbf{v},\mathbf{M}=\mathbf{m})&\\ \cdot P(\mathbf{V}=\mathbf{v}|\mathbf{M}=\mathbf{m})\cdot P(\mathbf{M}=\mathbf{m}).&\end{aligned} \tag{3}$$

However, to a valid vehicle dynamic state $\{\mathbf{m},\ \mathbf{v},\ \mathbf{t},\ \mathbf{x}\}$, the time constraint and distance constraint must be satisfied. Besides, the elements of $\mathbf{v}$, $\mathbf{t}$ and $\mathbf{x}$ are not less than zero because of nonnegative matrixes. They are

$$\begin{aligned}\Omega_V &= \{\mathbf{v}|v_1=v_2=u_1,v_K=v_{K+1}=u_2,v_i\geq 0,\\ &\quad K=3\ or\ 5\};\\ \Omega_T &= \{\mathbf{t}|t_1\geq 0,\ldots t_K\geq 0,\ K=3\ or\ 5\};\\ \Omega_X &= \{\mathbf{x}|x_1\geq 0,\ldots x_K\geq 0,\ K=3\ or\ 5\};\end{aligned} \tag{4}$$

$$\sum t_i=\Delta t;\ \sum x_i=\Delta d. \tag{5}$$

Based on the constraints above, Equation (6) is used to calculate the probability of a valid vehicle dynamic state.

$$P\left(\mathbf{M}=\mathbf{m},\mathbf{V}=\mathbf{v},\mathbf{T}=\mathbf{t},\mathbf{X}=\mathbf{x}\ \middle|\ \sum_{i=1}^{K_{\max}}T_i=\Delta t,\sum_{i=1}^{K_{\max}}X_i=\Delta d\right). \tag{6}$$

C. Vehicle Trajectory Reconstruction for Acceleration and Deceleration Modes

To a certain modal activity, if the mode is an acceleration mode or a deceleration mode, the starting speed (v_i), ending speed (v_{i+1}), time consumption (t_i) and traveling distance (x_i) are given. In Hao *et al.* [10], we assume that the acceleration rate of those modes follows a linear acceleration model with $a_{i,1}$ as the intercept and r_i as the slope, i.e.

$$a_i(t)=a_{i,1}+r_i t. \tag{7}$$

Based on the constrains of speed, time and distance, we have equation (8) and (9) to solve the values of $a_{i,1}$ and r_i.

$$\begin{cases}v_{i+1}=v_i+a_{i,1}\times t_i+\dfrac{1}{2}r_i\times t_i^2;\\ x_i=v_i\times t_i+\dfrac{1}{2}a_{i,1}\times t_i^2+\dfrac{1}{6}r_i\times t_i^3.\end{cases} \tag{8}$$

$$\begin{cases}r_i=\dfrac{6(v_i+v_{i+1})\times t_i-12x_i}{t_i^3};\\ a_{i,1}=\dfrac{v_{i+1}-v_i}{t_i}-\dfrac{1}{2}r_i\times t_i.\end{cases} \tag{9}$$

Therefore, the second-by-second speed/acceleration data can be estimated by substituting the calculated $a_{i,1}$ and r_i into equation (7) and (8).

D. Speed Oscillation Effect of Cruising Mode

Normally, a driver cannot keep a constant speed without speed fluctuation. Therefore, speed oscillation effect of cruising modal should be integrated to capture the real-world driving characteristics. Hao et al. proposed a new method to incorporate the speed oscillation effect, which is integrated in our model framework [11]. Assume the cruising modal traveling time is τ in second, where τ is an integer, $\tau\geq 2$. For each second, the acceleration rate α_i $(i=1,2,\ldots,\tau)$ is a normal random number, following Gaussian distribution $N(0,\sigma_c)$.

Firstly, we can generate $(\tau-1)$ independent normal random numbers following $N(0,\sigma_c)$, say β_i. And we can set that $\mathrm{B}=[\beta_1,\beta_2,\ldots,\beta_{\tau-1}]^{\mathrm{T}}$. Then we can use equation (10) to generate a vector $\mathrm{A}=[\alpha_1,\alpha_2,\ldots,\alpha_\tau]^{\mathrm{T}}$, which follows the Gaussian distribution $N(0,\sigma_c)$ and satisfy the constraint $(\sum_{i=1}^{\tau}\alpha_i=0)$.

$$\begin{aligned}\mathbf{A}&=\sigma\sqrt{\frac{\tau}{\tau-1}}\mathbf{Q}\mathbf{B};\\ \mathbf{e}^{\mathbf{T}}\mathbf{Q}&=0;\ \mathbf{Q}^{\mathbf{T}}\mathbf{Q}=\mathbf{I}.\end{aligned} \tag{10}$$

where $\mathbf{e}$ is a $1\times\tau$ all-one matrix; $\mathbf{Q}$ is a $\tau\times(\tau-1)$ all orthonormal basis matrix. The certification procedure can be seen in [11].

III. Vehicle Energy/Emissions Estimation Method

Micro vehicle energy/emissions modelling is first introduced using MOVES model. Then vehicle energy/emissions characteristics are estimated based on the reconstructed vehicle trajectory using sparse mobile sensor data.

A. Micro Vehicle Energy/Emissions Modeling

Vehicle energy/emissions features are estimated using MOVES 2014a. In MOVES model, a binning approach is applied to present different vehicle conditions including acceleration, deceleration, cruising and idling based on the distribution of calculated Vehicle Specific Power (VSP) for each second. The formula is as follows:

$$\mathrm{VSP}=\frac{A\times v}{Mass}+\frac{B\times v^2}{\mathrm{Mass}}+\frac{C\times v^3}{\mathrm{Mass}}+(a+g\times\sin\theta)\times v, \tag{11}$$

where VSP is in KW/ton; v is in m/s, a is in m/s^2; A, B, C, are the road load coefficients in units of kW/(m/s), kW/(m/s)^2, and kW/(m/s)^3, respectively. *Mass* means the fixed mass factor, g is the acceleration due to gravity (9.8 m/s^2), and $\sin\theta$ set to 0 assuming flat road.

Based on the results of VSP, vehicle operation mode distribution could be calculated for a specific vehicle at specific time. Then we can calculate vehicle emissions and fuel consumption based on the emission factors from MOVES database. Noted that we input the revised relevant factors in MOVES model to estimate vehicle energy/emissions, such as meteorological parameters and vehicle age distribution.

B. Vehicle Energy/Emissions Estimation

As stated in the above section, to a certain vehicle dynamic state $\{\mathbf{m}, \mathbf{v}, \mathbf{t}, \mathbf{x}\}$, the distance error ε can be calculated using equation (12). For a valid vehicle dynamic state, ε should be less than 1.5 meters when $\sum t_i = \Delta t$.

$$\varepsilon = \left| \sum x_i - \Delta d \right|. \tag{12}$$

Obviously, there may be some optional traffic states with the same values of probabilities. The reason is that for the cruising mode, the modal travel time and distance are assumed to be uniformly distributed. Therefore, we select the valid vehicle dynamic state with the least distance error. Even if the values of the distance errors are the same, we select a valid traffic state randomly. Thus, based on equation (6), we select the best scenario with the largest probability in a valid vehicle dynamic state in equation (13).

$$\max P\Bigg(\boldsymbol{M} = \boldsymbol{m}^*, \boldsymbol{V} = \boldsymbol{v}^*, \boldsymbol{T} = \boldsymbol{t}^*, \boldsymbol{X} = \boldsymbol{x}^*. \left| \sum_{i=1}^{K_{\max}} T_i = \Delta t, \sum_{i=1}^{K_{\max}} X_i = \Delta d \right)\Bigg). \tag{13}$$

Based on vehicle trajectory reconstruction, we can calculate the VSP characteristics of vehicles, and then estimate vehicle energy/emissions using MOVES model.

IV. Model Calibration

We first illustrate how we can divide the actual vehicle trajectory into four driving modes. Then, we use the historical data to generate different time interval data pair to calibrate the distribution of the inflection speed. After determining the acceleration or deceleration driving mode, we can also estimate the distribution parameters of time consumption and traveling distance during an acceleration or deceleration process. Finally, speed oscillation effect of cruising modal is calibrated using the cruising modal data.

A. Robust Driving Mode Segmentation for Ground Truth

In this paper, we use NGSIM U.S. 101 and Lankershim Blvd datasets with the second-by-second trajectories as the training dataset to learn the time and distance distribution parameters. As for the U.S. 101, the period from 08:05-8:20 is used as the model calibration dataset, and the dataset during the period from 08:20-08:35 is used for numerical experiments. The field observation site of U.S. 101 is approximately 640 m in length, with five mainline lanes throughout the section [12]. For the Lankershim Blvd, the model calibration dataset is from 08:30-08:45, and the dataset during the period from 08:45-09:00 is used for numerical experiments. There are 5 links and 4 intersections in the study corridor [13].

TABLE II
Calibration Results for Mode Segmentation

Road types	a_1	a_2	a_3	a_4	a_5	Min fitness
Unit	m/s^2	m/s	m/s^2	m/s	m/s	m/s^2
Freeways	0.33	1.01	0.49	1.49	0.39	2225.6
Arterial roads	0.29	1.03	0.29	0.88	0.44	1080.1

For the training dataset, we partitioned the second-by-second trajectory data into four driving modes. Intuitively, when the value of the vehicle's acceleration or deceleration rate is greater than zero, we may consider the vehicle is on acceleration or deceleration driving mode. Otherwise, the vehicle is on idling if the speed is zero or cruising mode if the speed is above zero. A driver cannot keep a constant speed without speed fluctuation, so a robust method should be adopted to partition the real-world vehicle trajectory data.

In our study, we assume that an acceleration driving mode is defined as a series of observations with instantaneous accelerations greater than a_1m/s^2, lasting for 3s or longer, and accumulating a speed increment greater than a_2 m/s. Similarly, a deceleration driving mode is defined as continuous observations with instantaneous decelerations (the absolute value) greater than a_3 m/s^2, lasting for 3s or longer, and accumulating a speed decrease greater than a_4 m/s. The remaining speed points are classified as cruising (speed larger than a_5 m/s) or idling driving mode (speed less than a_5 m/s). In order to achieve a robust segmentation, the genetic algorithm is used to calibrate the combination of these five parameters, (a_1, a_2, a_3, a_4, a_5). The number of population sizes is 20, the maximum number of iterations is 100, and the values of probability of crossover and mutation operations are 0.8 and 0.005. The function of fitness used to calculate the error is given by equation (14).

$$\text{Fitness} = w \times \sum \theta_1 + (1 - w) \times \sum \theta_2. \tag{14}$$

where θ_1 is the standard deviation of acceleration of any cruising event, which should be close to zero; θ_2 is the average acceleration of any cruise event, which should be small; and w is the weight for the objective of θ_1. In this study, w is set as 0.5. The calibrating ranges of these five parameters are [0.25 0.5] m/s^2, [0.75 1.5] m/s, [0.25 0.5] m/s^2, [0.75 1.5] m/s and [0.25 0.5] m/s. The calibration results are shown in Table II. Due to the signal intersections, vehicles driving on arterial roads have more acceleration and deceleration modes than vehicles driving on freeways resulting in the smaller threshold values of a_1 and a_3. For cruising mode, the value of a_5 on freeways is a little smaller than the value on arterial roads.

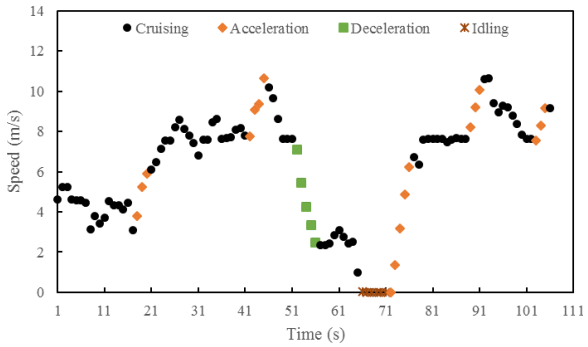

Fig. 5. Typical partitioning result of a vehicle on freeway.

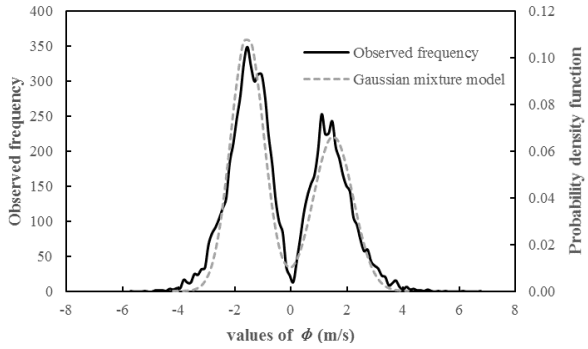

Fig. 6. Observed frequency of the values of $\phi = \hat{v} - \bar{v}$.

The combination parameters allow for representation of the natural variability in driving patterns happening in real world. The minor acceleration and deceleration modes can be identified during cruise operation modes; a typical partitioning result on freeway is illustrated in Fig. 5.

B. Probability Estimation of Inflection Speed Point

Based on NGSIM U.S. 101 dataset, we can generate numerous different time interval data pairs and find that the gap between the inflection speed $\hat{v}$ and average speed $\bar{v}$ implies a bimodal distribution. For example, for 10 s time interval on freeway data, Fig. 6 shows the observed frequency distribution of speed gap $\hat{v} - \bar{v}$ (denoted as ϕ). Two peaks are found in the plot, with the values of -1.54 m/s and 1.11 m/s respectively. The minimum and maximum values of ϕ are -4.82 m/s and 5.01 m/s respectively.

A Gaussian Mixture Model (GMM) is then adopted to learn the probability of ϕ. The probability density functions of ϕ and $\hat{v}$ are formulated as follows:

$$P(\phi) = \sum_{g=1}^{G} \pi_g P(\phi|g), \tag{15}$$

$$P(\hat{v}) = P(\bar{v} - \phi) = P(\phi) = \sum_{g=1}^{G} \pi_g P(\phi|g), \tag{16}$$

where g is the index of Gaussian distributions; π_g is the weighting factor associated with the g-th Gaussian distribution $N(q_g, \sigma_g)$ and $\sum_{g=1}^{G} \pi_g = 1$.

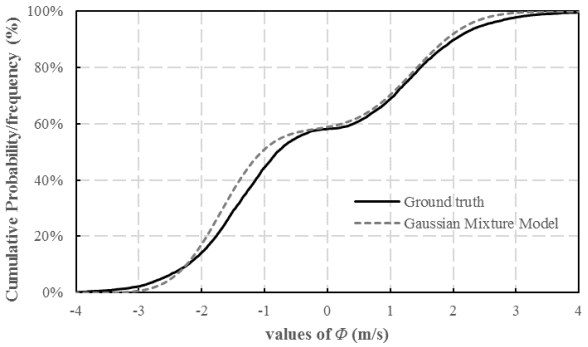

Fig. 7. Cumulative probability of GMM for 10 s time interval.

TABLE III
PARAMETERS FOR GMM WITH THE DIFFERENT TIME INTERVALS ON FREEWAYS

Δt	q_1	q_2	π_1	π_2	σ_1	σ_2
10	-1.886	1.976	0.596	0.404	0.382	0.415
15	-2.591	2.579	0.618	0.382	0.715	0.783
20	-3.142	2.976	0.613	0.387	0.958	1.059
25	-3.595	3.276	0.609	0.391	1.188	1.183
30	-3.993	3.546	0.613	0.387	1.405	1.147

TABLE IV
PARAMETERS FOR OR GMM WITH THE DIFFERENT TIME INTERVALS ON ARTERIAL ROADS

Δt	q_1	q_2	π_1	π_2	σ_1	σ_2
10	-2.385	2.420	0.438	0.562	0.999	0.880
15	-3.244	3.205	0.449	0.551	2.123	1.928
20	-3.811	3.858	0.448	0.552	3.411	2.820
25	-4.228	4.562	0.449	0.551	4.404	3.354
30	-4.439	5.418	0.471	0.529	5.482	3.249

Based on the observation from Fig. 6, we set $G = 2$. Then maximum likelihood method was applied to calibrate the values of π_g, q_g, σ_g.

$$\max \sum_{i} \log\Big(\sum_{g=1}^{G} \pi_g N(\phi_i|q_g, \sigma_g)\Big). \tag{17}$$

Expectation maximization algorithm is used to solve equation (17). Cumulative distribution functions of GMM and ground truth for 10 s time interval are plotted in Fig. 7 to illustrate the accuracy of the GMM model results. The parameters of GMM for different time interval on different road types are listed in Table III and Table IV.

As can be seen in Table III and Table IV, for different road types, we find that the values of q_1 and q_2 reflecting the gaps with largest probabilities between the inflection speed and average speed on a freeway are less than the values of arterial roads at the same time interval. The reason may be that traffic flow on freeways like a continuous fluid which is not interrupted by intersections or crossings.

TABLE V
CALIBRATION RESULTS FOR ACCELERATION AND DECELERATION MODES

Mode	Parameters	Freeway		Arterial Road	
		u_d	σ_d	u_d	σ_d
Acceleration	ξ	1.080	0.314	0.814	0.311
	Φ	0.464	0.040	0.419	0.107
Deceleration	ξ	1.164	0.350	1.099	0.582
	Φ	0.411	0.052	0.431	0.074

C. Distribution Parameters of Different Driving Modals

We assume the acceleration pace (i.e., 1/ acceleration) follows Gaussian distribution, so the travel time t that a vehicle has spent under the acceleration mode is the product of speed variation Δv multiplied by a Gaussian multiplier [10].

$$\xi = \frac{t}{\Delta v} \sim N(\mu_t, \sigma_t). \tag{18}$$

After partitioning of the speed-time profile, we can record the mode travel time and Δv during acceleration/deceleration driving mode using historical data. So parameters of u_t and σ_t of the Gaussian distribution $N(u_t, \sigma_t)$ could be estimated via maximum likelihood estimation. We then assume that the distance d that a vehicle travels under the acceleration/deceleration mode follows:

$$\begin{cases} d = t \times (v_s + v_e)\Phi, \\ \Phi = \dfrac{d}{t \times (v_s + v_e)} \sim N(\mu_d, \sigma_d), \end{cases} \tag{19}$$

where v_s and v_e are the instant speed at the start and end of the mode respectively. If the acceleration process follows constant acceleration motion, $d = t \times (v_s + v_e)/2$. Another Gaussian distribution $\Phi \sim N(u_d, \sigma_d)$ is set to measure how far the acceleration process deviated from the constant acceleration motion [10]. The parameters u_d and σ_d of the Gaussian distribution $N(u_d, \sigma_d)$ could also be estimated using maximum likelihood estimation. Table V shows the calibrated parameters of acceleration and deceleration process in this model.

From Table V, we can find that the average accelerating and decelerating rates of a vehicle driving on a freeway are less than the values of a vehicle driving on an arterial road. The values of Φ are around 0.45 rather than 0.5, which means the process of acceleration mode or deceleration mode do not follow the constant acceleration or constant deceleration process.

For speed oscillation effect of cruising mode, we assume the accelerating rate of cruising modal follows a Gaussian distribution $N(0, \sigma_c)$. Based on the partitioning results of real-world vehicle trajectories, the calibrated value of σ_c is 0.4 m/s^2 on freeways, which doubles on arterial roads with the value of 0.2 m/s^2. That means the speed of cruising mode on freeways fluctuates more significantly than speed on arterial roads.

V. NUMERICAL EXPERIMENTS

Numerical experiments are conducted using the other period NGSIM dataset. Vehicle trajectories are first reconstructed. Vehicle energy/emissions factors are then estimated using MOVES model. Sensitivity analysis is performed to show the model accuracy with different time intervals.

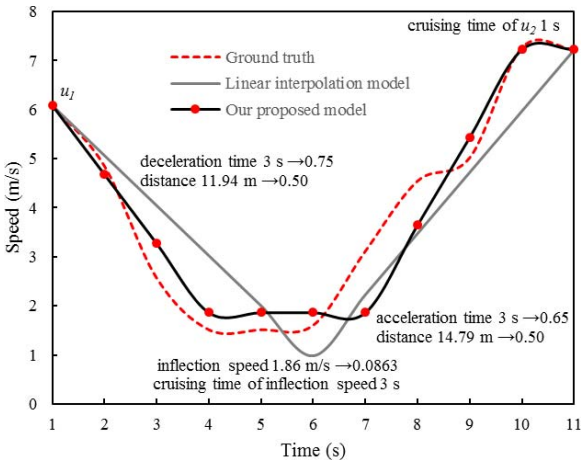

Fig. 8. A case study of a sparse mobile sensor data pair.

A. Vehicle Trajectory Reconstruction

Based on the proposed modal activity-based vehicle trajectory estimation model, a case study of vehicle trajectory reconstruction to a example data pair is shown in Fig. 8.

Fig. 8 illustrates the process to estimate the probability of a certain sparse mobile sensor data pair. The sample time interval is 10 s and the distance between two samples is 38.23 m, with the starting and ending speed of 6.09 m/s and 7.23 m/s. For the scenario with the largest probability, there is an inflection speed point with the value of 1.86 m/s. The estimated time periods of deceleration and acceleration mode are 3 s and 3 s. The estimated distances of deceleration and acceleration mode are 11.94 m and 10.88 m. To the cruising assignment, 3 s are allocated to the location of $\hat{v}$, and 1 s is allocated to the location of u_2. The value of ε reflecting the distance error between estimated value and real-world distance is 0.17 m less than 1.5 m, see equation (12). Thus, we can compute the conditional probability of the extreme speed, acceleration/deceleration mode time and distance. The probability of this valid scenario is the product of all the conditional probabilities, as follows:

$$P = 1 \times 0.0863 \times 0.75 \times 0.5 \times 0.65 \times 0.5 = 0.0105. \tag{20}$$

To the same data pair, we also apply the linear interpolation method as a baseline model to reconstruct the vehicle trajectory. The baseline model simply assumes that the acceleration time is equal to the deceleration time. No cruising or idling mode is considered during vehicle trajectory reconstruction. The Mean Absolute Error (MAE) of our proposed model on second-by-second location estimation is 0.51 m, while the MAE of the baseline model is 2.89 m. Besides, the MAE of the proposed model on second-by second speed is 0.40 m/s, which is almost half of the linear interpolation model (0.71 m/s). Results show that the proposed model outperforms the linear interpolation model due to the consideration of traffic domain knowledge, named the driving mode sequence and inflection speed point distribution.

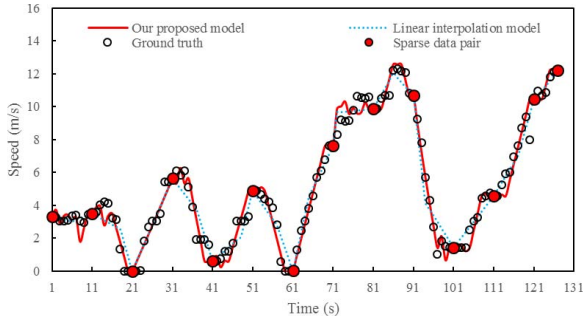

Fig. 9. Results of a certain vehicle trajectory reconstruction.

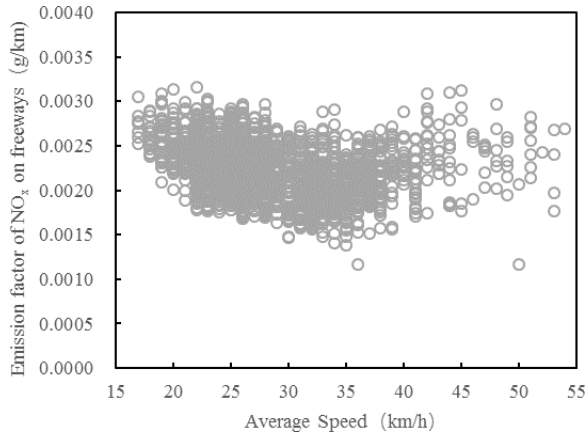

Fig. 10. Estimated emission factors of NOx with 10 s time interval.

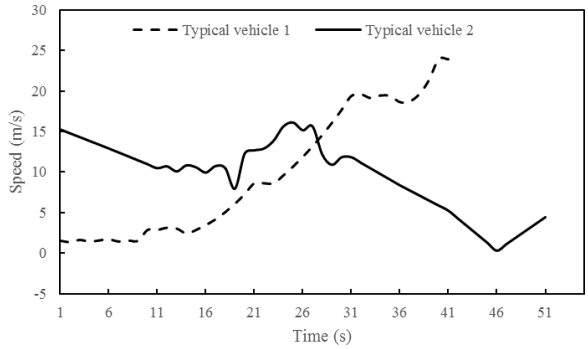

Fig. 11. Typical vehicle trajectories at the speed of 35 km/h.

Fig. 9 shows the result of the example vehicle speed-time trajectory estimation in the study area assuming 10 s time interval. Overall, the estimated trajectories considering speed oscillation effect matches the observations very well. The accumulative total absolute speed error of all the time for this vehicle trajectory estimation using our model is 54.58 m/s, while the value of linear interpolation model is 101.43 m/s. The proposed model shows good performance compared with the ground truth due to the consideration of traffic domain knowledge, named the driving mode sequence and inflection speed point distribution.

B. Vehicle Energy/Emissions Estimation

After vehicle trajectory reconstruction, we can further estimate vehicle energy/emissions using MOVES model. For example, we estimate the NO_x emission (including nitric oxide and nitrogen dioxide) with 10 s time interval on freeways,

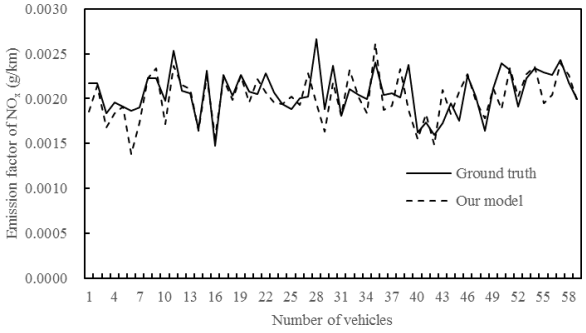

Fig. 12. Estimated emission factors at the same average speed.

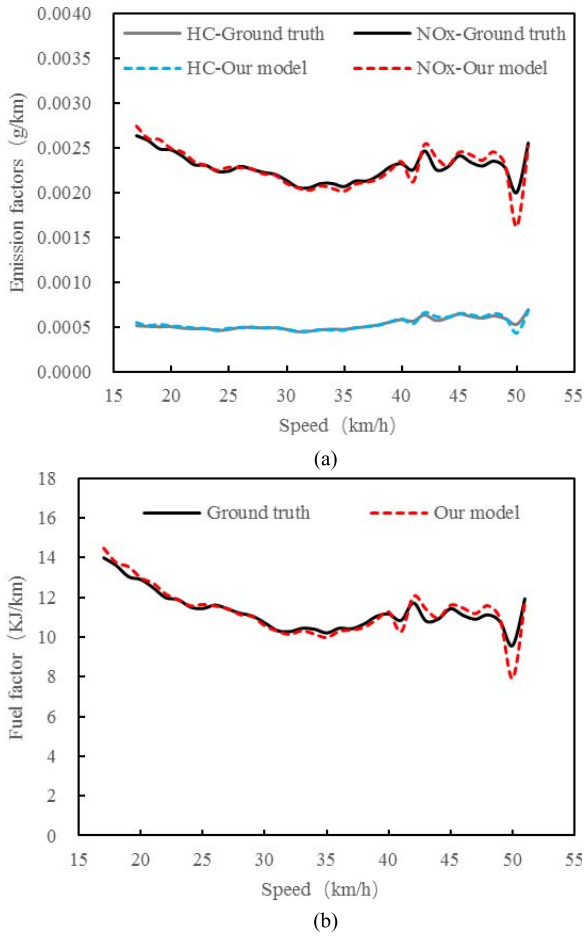

Fig. 13. Vehicle energy/emissions estimation on freeways. (a) Vehicle emission factors estimation. (b) Vehicle energy factor estimation.

as shown in Fig. 10. In general, The NO_x emission first shows a decreasing trend with decreasing speed and later increases with increasing speed. Meanwhile, vehicle emission factors are different even the vehicle average speed are the same due to the diversity of vehicle trajectories and modal activities. In Fig. 11, two vehicles' average speeds are around 35 km/h with different driving modes. The main driving modes of typical vehicle 1 are cruising and accelerating, while the other vehicle's driving modes are cruising and decelerating, resulting in the different emission factors at the same average traveling speed.

To illustrate the accuracy of the proposed model, we compare the estimated NO_x emission factor and the ground truth

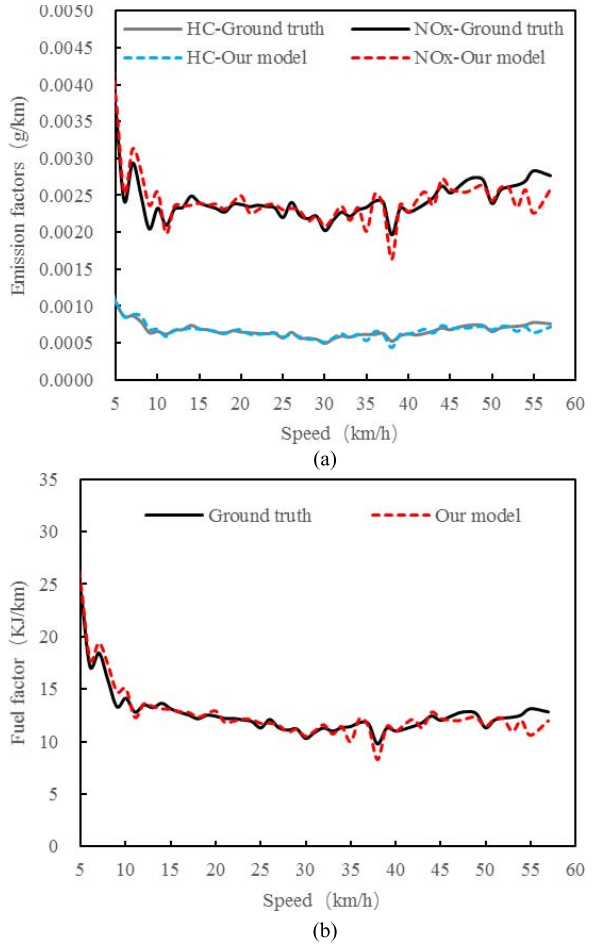

Fig. 14. Vehicle energy/emissions estimation on arterial roads. (a) Vehicle emission factors estimation. (b) Vehicle energy factor estimation.

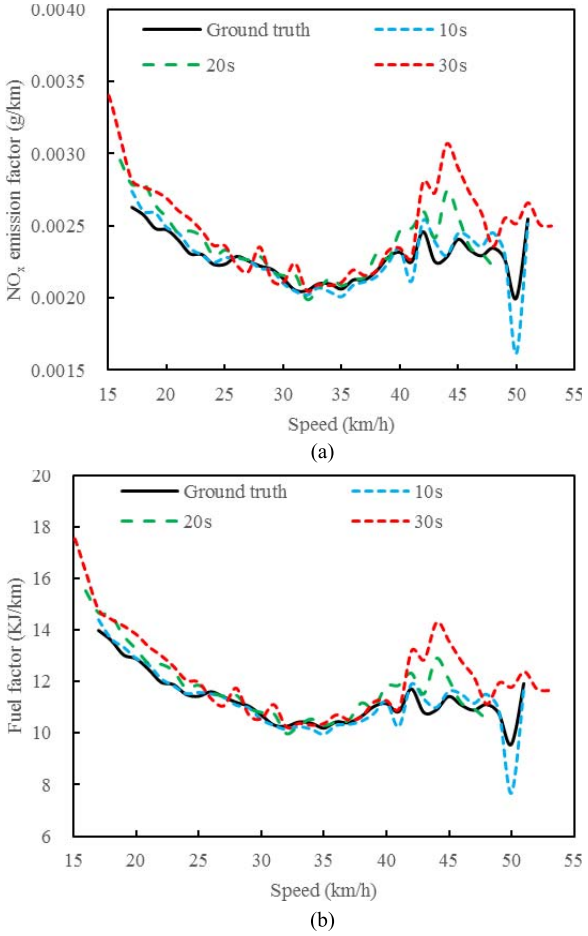

Fig. 15. Vehicle energy/emission estimation with different time intervals on freeways. (a) Vehicle NO_x emission factor estimation. (b) Vehicle energy factor estimation.

emission factor of all vehicles with the same average speed of 35 km/h, see Fig. 12. Noted that the ground truth emission factors are computed using the observed trajectories based on MOVES model. Results show that our model can well distinguish vehicle emission factors of different vehicles even vehicles at the same average speed.

To measure the accuracy of our model at the different traveling speed, we calculate the average estimated energy/emission factors at the same speed compare with the ground truth on different types of roads, see Fig. 13 and Fig. 14. Overall, our model can estimate vehicle energy/emissions characteristics precisely through vehicle trajectory reconstruction.

We define the Mean Absolute Percentage Error (MAPE) to represent the errors between model estimation results and ground truth with the consideration of different vehicle emissions factors, as follows:

$$\text{MAPE} = \frac{\sum |(e_t - \hat{e}_t)/e_t|}{n}, \tag{21}$$

where $\hat{e}_t$ is the estimated vehicle fuel/emissions factors, such as HC, CO, NO_x, CO_2 and fuel consumption; e_t is the ground truth factors; n is the total samples.

To arterial roads, the MAPE of energy factor is only 3.6%, the MAPE values of HC and NO_x are 3.9% and 4.2%. The MAPEs for freeways are 2.4%, 2.8% and 2.7%, respectively.

TABLE VI

MAPEs OF VEHICLE ENERGY/EMISSIONS FACTORS WITH THE DIFFERENT TIME INTERVALS

Factor	Freeway			Arterial road		
	10 s	20 s	30 s	10 s	20 s	30 s
HC	2.7%	6.1%	9.9%	3.9%	4.0%	10.3%
CO	3.7%	8.0%	12.8%	5.5%	5.2%	12.8%
NO_x	2.5%	6.3%	10.3%	4.2%	7.6%	17.9%
Energy	2.3%	5.5%	9.0%	3.6%	6.5%	14.1%

Moreover, there is lack of extreme congestion on freeways when traveling speed is less than 15 km/h, see Fig. 13. Vehicle energy/emissions factors on arterial roads show a little larger than these factors on freeways at a certain speed due to the influence of intersections.

C. Sensitivity Analysis With Different Time Intervals

Effects of different time intervals of our model are also analyzed. We set that time interval varies from 10 s to 30 s, see Fig. 15 and Fig. 16. We also calculate the MAPEs of vehicle energy/emissions factors at the different time intervals, as shown in Table VI. Overall, with the increasing of time interval of sparse mobile sensor data, the MAPEs of vehicle energy/emissions factors show an increasing trend for freeways and arterials.

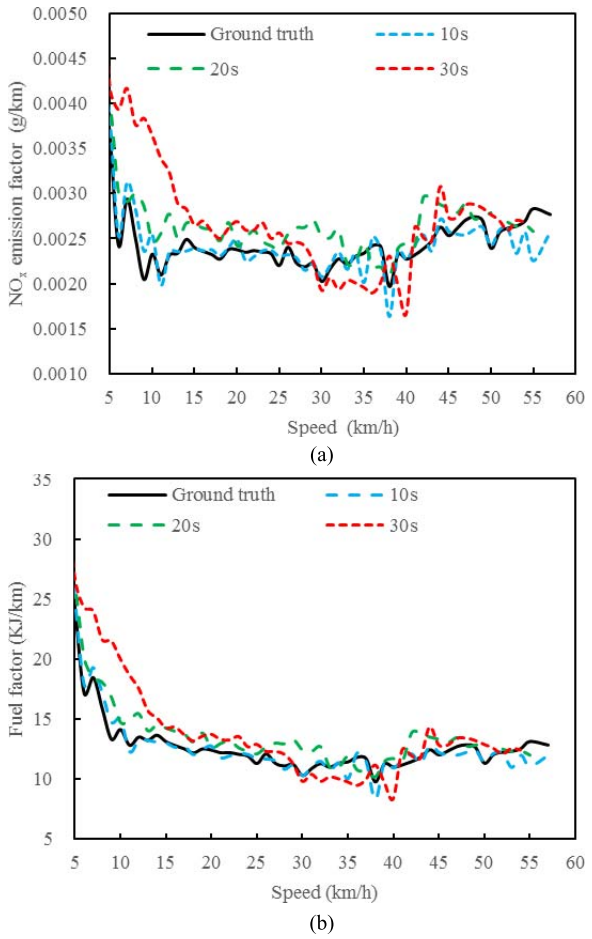

Fig. 16. Vehicle energy/emission estimation with different time intervals on arterial roads. (a) vehicle NO_X emission factor estimation. (b) vehicle energy factor estimation.

TABLE VII

MAPEs OF VEHICLE ENERGY/EMISSIONS FACTORS FOR THE DIFFERENT MODELS WITH 20 s TIME INTERVAL

factors	Freeway		Arterial	
	Our proposed model	Linear interpolation model	Our proposed model	Linear interpolation model
HC	6.1%	6.3%	4.0%	4.7%
CO	8.0%	8.8%	5.2%	6.2%
NO_x	6.3%	7.2%	7.6%	9.1%
Energy	5.5%	6.1%	6.5%	7.6%

As can be seen from Table VI, our mode performs good estimation on vehicle energy/emissions factors when the time interval is less than 20 s. In these cases, the MAPEs of all vehicle energy/emissions factors are less than 8%. When the time interval is 30 s, estimated vehicle energy/emissions factors shows greater variation around ground truth data, especially when the traveling speed is around 40-50 km/h on freeways and the speed less than 15 km/h on arterials. It means that model assumption may be not consistent with the actual driving characteristics with 30 s time interval. For example, there may be two or more inflection speed points with large time intervals rather than only one inflection speed point assumption between a certain sparse data pair.

D. Performance Comparison Between Our Proposed Model and Linear Interpolation Model

To illustrate the advantages of the trajectory reconstruction strategy, the estimation results of our proposed model are compared with the estimate results of linear interpolation model with 20 s time interval, as shown in Table VII. Linear interpolation model can reflect the characteristics of velocity fluctuation at a certain level [7], resulting in the MAPEs of vehicle energy/emissions factors less than 10%. Our proposed model shows better estimation performance, with the values of MAPEs less then 8%.

VI. CONCLUSIONS

This study proposed a new framework of vehicle energy/emissions estimation based on vehicle trajectory reconstruction using sparse mobile sensor data. Methodology of modal activity-based vehicle trajectory reconstruction is proposed with consideration of traffic domain knowledge. Then vehicle energy/emissions are estimated based on operating mode distribution using MOVES model. Model calibrations are conducted using NGSIM dataset. Numerical experiments including vehicle trajectory reconstruction, vehicle energy/emissions estimation are analyzed and compared with ground truth. The numerical results show good performance on vehicle operating mode distribution and vehicle energy/emissions estimation. Besides, sensitivity analysis with different time interval are also explored to illustrate the accuracy of our proposed model.

The results reveal that modal activity-based model can capture the actual features of different driving mode. Speed oscillation effect has a significant influence on vehicle energy/emissions estimation. With the increase of time interval, the MAPEs of vehicle energy/emissions factors show an increasing trend. When the time interval is 30 s, the estimation fluctuates significantly around the ground truth due to the limitation of model assumption.

In the proposed research, due to the computational complexity, we assume that there is only one inflection speed point during the time interval period. It is reasonable when the time interval is less than 30 s. New modal activity-based method on vehicle trajectory reconstruction which considering more than one inflection speed point should be proposed for the cases with larger time interval.

In this paper, we validate our model using the other period NGSIM dataset. More vehicle trajectory data should be collected on other roads to validate the accuracy of our model. Besides, due to the different vehicle types with different driving features, such as buses, Our model can be applied to sparse bus data to estimate bus energy/emissions characteristics. Furthermore, the impact of the quality of observation data on the performance of our model should be investigated, such as the GPS positioning errors. The authors recommend that future research could focus on those issues.

REFERENCES

[1] *Comprehensive Modal Emission Model (CMEM).* Accessed: Feb. 6, 2017. [Online]. Available: http://www.cert.ucr.edu/cmem/

[2] *MOVES and Other Mobile Source Emissions Models*. Accessed: Dec. 19, 2016. [Online]. Available: https://www.epa.gov/moves
[3] C. A. Quiroga and D. Bullock, "Travel time studies with global positioning and geographic information systems: An integrated methodology," *Transp. Res. C, Emerg. Technol.*, vol. 6, nos. 1–2, pp. 101–127, Feb. 1998.
[4] K. Liu, T. Yamamoto, and T. Morikawa, "Estimating delay time at signalized intersections by probe vehicles," in *Proc. 5th Int. Conf. Traffic Transp. Stud.*, 2006, pp. 644–655.
[5] R. Herring, A. Hofleitner, P. Abbeel, and A. Bayen, "Estimating arterial traffic conditions using sparse probe data," in *Proc. IEEE Intell. Transp. Syst. Conf.*, Sep. 2012, pp. 929–936.
[6] X. Wang, L. Peng, T. Chi, M. Li, X. Yao, and J. Shao, "A hidden Markov model for urban-scale traffic estimation using floating car data," *PLos ONE*, vol. 10, no. 12, p. e0145348, 2015.
[7] H. Liu, X. Chen, Y. Wang, and S. Han, "Vehicle emission and near-road air quality modeling for Shanghai, China: Based on global positioning system data from taxis and revised MOVES emission inventory," *Transp. Res. Rec., J. Transp. Res. Board*, vol. 2340, pp. 38–48, Sep. 2013.
[8] X. Zhou *et al.*, "Integrating a simplified emission estimation model and mesoscopic dynamic traffic simulator to efficiently evaluate emission impacts of traffic management strategies," *Transp. Res. D, Transp. Environ.*, vol. 37, pp. 123–136, Jun. 2015.
[9] S. K. Zegeye, B. De Schutter, J. Hellendoorn, E. A. Breunesse, and A. Hegyi, "Integrated macroscopic traffic flow, emission, and fuel consumption model for control purposes," *Transp. Res. C, Emerg. Technol.*, vol. 31, pp. 158–171, Jun. 2013.
[10] P. Hao, K. Boriboonsomsin, G. Wu, and M. Barth, "Modal activity-based stochastic model for estimating vehicle trajectories from sparse mobile sensor data," *IEEE Trans. Intell. Transp. Syst.*, vol. 18, no. 3, pp. 701–711, Mar. 2017.
[11] P. Hao, G. Wu, K. Boriboonsomsin, and M. Barth, "Modal activity-based vehicle energy/emissions estimation using sparse mobile sensor data," in *Proc. Transp. Res. Board Annu. Meeting*, 2016, p. 6861.
[12] *U.S. Highway 101 Dataset*. Accessed: Sep. 8, 2017. [Online]. Available: https://www.fhwa.dot.gov/publications/research/operations/07030/index.cfm
[13] *Lankershim Boulevard Dataset*. Accessed: Sep. 8, 2017. [Online]. Available: https://www.fhwa.dot.gov/publications/research/operations/07029/index.cfm

Xiaonian Shan received the B.S. degree from Southeast University, Nanjing, China, in 2012. He is currently pursuing the Ph.D. degree with Tongji University. From 2015 to 2016, he was a Visiting Ph.D. Student with the Bourns College of Engineering–Center for Environmental Research and Technology, University of California at Riverside, Riverside. His research interests include vehicle energy and emissions modeling, managed lane design, traffic operation management, and intelligent transportation systems.

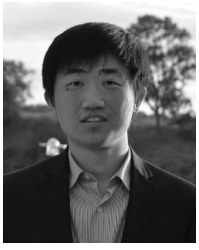

Peng Hao (M'16) received the B.S. degree in civil engineering from Tsinghua University in 2008 and the Ph.D. degree in transportation engineering from Rensselaer Polytechnic Institute in 2013. He is currently a Post-Doctoral Scholar with the Center for Environmental Research and Technology, College of Engineering, University of California at Riverside, Riverside. His research interests include connected vehicles, eco-approach and departure, sensor-aided modeling, signal control, and traffic operations. He is a member of the IEEE Intelligent Transportation System Society, the Institute for Operations Research and the Management Sciences, and Chinese Overseas Transportation Association.

Xiaohong Chen received the D.Eng. degree from the School of Traffic and Transportation Engineering, Tongji University, in 2003. She has published over 20 papers in peer-reviewed journals. She has made a long-term commitment to the basic and frontier research work of regional comprehensive transportation system planning, road network planning, public transit system planning, and pedestrian and bicycle transport systems. Her research includes transportation planning systems and methodology for metropolitan and rapid urbanization areas, transportation environment, basic theory and planning methods for pedestrian and bicycle traffic flow, and new energy transportation system planning.

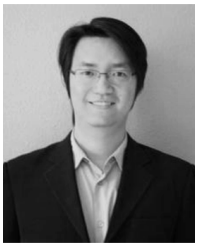

Kanok Boriboonsomsin (M'14) received the Ph.D. degree in transportation engineering from University of Mississippi, Oxford, MS, USA, in 2004. He is currently an Associate Research Engineer with the Center for Environmental Research and Technology, College of Engineering, University of California at Riverside, Riverside, USA. His research interests include sustainable transportation systems and technologies, intelligent transportation systems, traffic simulation, traffic operations, transportation modeling, vehicle emissions modeling, and vehicle activity analysis. He is a member of the Transportation and Air Quality Standing Committee of Transportation Research Board and the Institute of Transportation Engineers. He serves as an Associate Editor for IEEE *Intelligent Transportation Systems Magazine*.

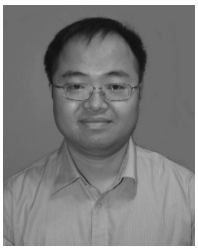

Guoyuan Wu (M'09–SM'15) received the Ph.D. degree in mechanical engineering from University of California at Berkeley, Berkeley, in 2010. From 2005 to 2010, he was a Graduate Student Researcher with California Partners for Advanced Transportation Technology. He is currently an Assistant Research Engineer with the Transportation Systems Research Group, Center for Environmental Research and Technology, Bourns College of Engineering, University of California at Riverside. His research focuses on intelligent and sustainable transportation system technologies, optimization and control of transportation systems, and traffic simulation. He is also a member of the Institute of Transportation Engineers and Chinese Overseas Transportation Association.

Matthew J. Barth (M'90–SM'00–F'14) received the B.S. degree in electrical engineering/computer science from University of Colorado in 1984, and the M.S. and Ph.D. degrees in electrical and computer engineering from University of California at Santa Barbara, Santa Barbara, in 1985 and 1990, respectively. He joined University of California at Riverside (UCR), Riverside, in 1991, conducting research in intelligent systems, where he is currently the Yeager Families Professor with the College of Engineering. He is also with the Intelligent Systems Faculty in electrical and computer engineering and also is the Director of the Center for Environmental Research and Technology, UCR's largest multidisciplinary research center.

His research focuses on applying engineering system concepts and automation technology to transportation systems, and in particular how it relates to energy and air quality issues. His current research interests include ITS and the environment, transportation/emissions modeling, vehicle activity analysis, advanced navigation techniques, electric vehicle technology, and advanced sensing and control.

Dr. Barth has also been active in the IEEE Intelligent Transportation System Society for many years, participating in conferences as a presenter, an invited session organizer, a session moderator, a reviewer, an Associate Editor of TRANSACTIONS OF INTELLIGENT TRANSPORTATION SYSTEMS, and a member of the IEEE ITSS Board of Governors. He was the IEEE ITSS Vice President for Conferences from 2011 to 2012, President-Elect for 2013, and the IEEE ITSS President from 2014 to 2015.